Journal of Medicinal Chemistry

Brief Article

Peptide-Boronic Acid Inhibitors of Flaviviral Proteases: Medicinal Chemistry and Structural Biology

Christoph Nitsche, Linlin Zhang, Lena F. Weigel, Jonas Schilz, Dominik Graf, Ralf Bartenschlager, Rolf Hilgenfeld, and Christian D. Klein

J. Med. Chem., **Just Accepted Manuscript** • DOI: 10.1021/acs.jmedchem.6b01021 • Publication Date (Web): 28 Nov 2016

ACS Publications

Journal of Medicinal Chemistry is published by the American Chemical Society. 1155 Sixteenth Street N.W., Washington, DC 20036

Peptide-Boronic Acid Inhibitors of Flaviviral Proteases: Medicinal Chemistry and Structural Biology

Christoph Nitsche,[†,‡] Linlin Zhang,[§,∥] Lena F. Weigel,[†] Jonas Schilz,[§] Dominik Graf,[†] Ralf Bartenschlager,[∥,⊥] Rolf Hilgenfeld,[§,∥] Christian D. Klein*[,†]

[†]Medicinal Chemistry, IPMB, Heidelberg University, INF-364, 69120 Heidelberg, Germany

[§]Institute of Biochemistry, Center for Structural and Cell Biology in Medicine, University of Lübeck, Ratzeburger Allee 160, 23562 Lübeck, Germany

[∥]German Center for Infection Research (DZIF), sites Hamburg - Lübeck - Borstel and Heidelberg

[⊥]Department of Infectious Diseases, Molecular Virology, Heidelberg University, INF-345, 69120 Heidelberg, Germany

ABSTRACT: A thousand-fold affinity gain is achieved by introduction of a C-terminal boronic acid moiety into dipeptidic inhibitors of the Zika, West Nile and dengue virus proteases. The resulting compounds have K_i values in the two-digit nanomolar range, are not cytotoxic, and inhibit virus replication. Structure-activity relationships and a high resolution X-ray co-crystal structure with West Nile virus protease provide a basis for the design of optimized covalent-reversible inhibitors aimed at emerging flaviviral pathogens.

INTRODUCTION

Infections with flaviviruses such as dengue, West Nile, and Zika virus are an increasing global health concern. With spreading habitats of the transmitting mosquitoes, infections and epidemics caused by these flaviviruses are a potential threat for previously unaffected regions such as Europe and Northern America. The recent Zika virus outbreak in South America has been declared as Public Health Emergency of International Concern by the WHO.

Enzyme inhibitors with a covalent binding mode[1] currently experience a remarkable revival in medicinal chemistry within a large variety of disease and target classes. The beta-lactam antibiotics, fosfomycin, aspirin and proton-pump inhibitors are long-established examples of drugs with a covalent binding mode and a convincing clinical activity and safety profile. Newly developed covalent inhibitors entered clinical practice, for example, in the kinase[2, 3] and proteasome fields,[4, 5] and have recently shown promise as inhibitors of serine carbapenemases.[6] From a chemical perspective, these compounds include potentially reactive functional groups such as boronic acid, acrylamide or epoxide that are otherwise considered highly unusual in drugs. The introduction of as-yet underexplored elements and building blocks into medicinal chemistry obviously represents a highly valuable strategy.

We here present an example in which the inclusion of a boronic acid moiety into peptidic inhibitors of flaviviral proteases led to a thousand-fold increase of affinity. The resulting compounds show efficacy in cell-culture models of dengue (DENV) and West Nile virus (WNV) replication and are not cytotoxic. The high affinity of the compounds also allowed the co-crystallization with the target proteases, yielding the first X-ray structures of a small-molecule, drug-like inhibitor covalently bound to West Nile and Zika virus proteases that enable the rational design of further derivatives with even higher potency. It should also be noted that haptenization and subsequent allergic reactions are not expected to be an issue with boronic acids, since they bind to biomacromolecules in a reversible-covalent manner.

Previous work by several groups[7-12] had indicated that compounds containing basic residues which resemble the polybasic substrate recognition profile of the flaviviral proteases display modest affinities in the micromolar range. In comparison, extension of these compounds towards the N-terminus and in the area of the P1 residue, as reported recently, resulted in peptidic inhibitors of the DENV and WNV proteases with activity in the lower nanomolar range.[13-16] However, the size ($M_r \approx 750$ Da) and basicity of these compounds present a problematic liability for further optimization and pharmacokinetics. We therefore considered it desirable to obtain alternative and smaller compounds in which these design factors are in a more attractive range. Considering a previous report,[17] in which a single boronic acid–tetrapeptide analog was reported as promising (K_i = 0.043 μM) but not studied in more detail, we set out to explore the potential of reversible-covalent dipeptide-boronic acid inhibitors of flaviviral proteases and elucidate their structure-activity relationships.

RESULTS AND DISCUSSION

The chemistry behind the present SAR dataset involved stereoselective preparation of the key intermediate **9** by Matteson homologation using the (+)-pinanediol ester as described previously (SI).[18-21] The further synthesis is based on a chiral-pool approach for the preparation of benzoyl-capped unnatural amino acids **10–15** (Scheme S2, SI), followed by fusion to precursor **9** (Scheme S1) and subsequent multi-step conversion of the side chain bromine to a guanidine function (Scheme 1).

The syntheses of the monopeptide-boronic acids **1** and **2** from **9** are outlined in the supporting information (Scheme S1, SI). The dipeptide-boronic acids **3–8**, containing various aromatic bioisosters for the basic P_2 side chain, were prepared from acids **10-15** according to Scheme 1. Coupling towards precursor **9** was successful in moderate yields, using the isobutyl mixed anhydride approach. The bromine intermediates were converted into the corresponding azides, the compounds were hydrogenated and finally transformed into the di(Boc)-protected guanidines.

The two guanidino groups in compounds **6–8** could be introduced simultaneously within one synthetic step after parallel reduction of the nitro and azido groups. This combined transformation crucially reduced the number of synthetic steps and improved the yield. For final deprotection, all remaining Boc groups were cleaved using TFA. The boronic acids **1-8** were subsequently released from pinanediol with an excess of phenylboronic acid in a two-phase mixture of water and diethyl ether.

Scheme 1. Synthesis of dipeptide-boronic acids.[a]

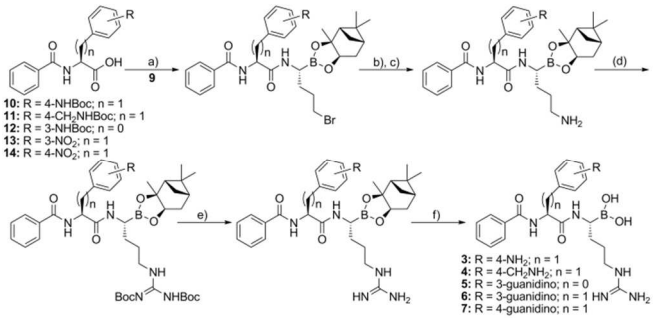

[a]Reagents and conditions: (a) NMM, IBCF, DIPEA THF, DCM, –15 °C; (b) NaN_3, DMF, 100 °C; (c) H_2, Pd/C, MeOH; (d) bis-Boc-pyrazole-1-carboxamidine, DMAP, MeOH; (e) TFA, DCM, HCl; (f) $PhB(OH)_2$, water, diethyl ether, HCl (aq.). The dipeptide **8** was synthesized in analogy to **7** from precursor **15** with a *t*Bu group in *para*-position. Step (c) was performed under acidic conditions (aqueous HCl) during synthesis of compounds **5–8**. All final compounds were isolated as hydrochloride salts.

Table 1. Activity data. Inhibitory activity of peptidyl-amides and -boronic acids against viral proteases and inhibition of dengue and West Nile virus replication by the peptidyl-boronic acids in cell culture.

Cpd. ID	Structure	Inhibition of DENV protease[a]		Inhibition of WNV protease[b]		Inhibition of ZIKV protease[c]	Cellular activity of the boronic acids (X=B(OH)$_2$)		
for X = B(OH)2		X = replacement of the terminal Arg/Orn carboxyl group; K_i and IC50 values in μM; % inhibition values at [inhibitor] = 50 μM					Cyto-toxicity[d]	Antiviral effect EC_{50} (μM)[e]	
		X = $CONH_2$	X = $B(OH)_2$	X = $CONH_2$	X = $B(OH)_2$	X = $B(OH)_2$	CC_{50} (μM)	DENV	WNV
1	Bz-Orn-X	2.0%	8.3%	18%	30%	IC_{50} > 50	> 100	7.5%	33%
2	Bz-Arg-X	9.7%	51.9%	9.6%	18%	IC_{50} > 50	> 100	12%	19%
3	Bz-(4-NH_2)Phe-Arg-X	5.2%	IC_{50} = 7.4 K_i = 4.2	13%	IC_{50} = 7.4 K_i = 6.0	IC_{50} > 40	10.1	44% (3.1 μM)	EC_{50} = 1.5
4	Bz-[4-(CH_2NH_2)]Phe-Arg-X	6.6%	IC_{50} = 0.066[f] K_i = 0.051[f]	20%	IC_{50} = 0.11[g] K_i = 0.082[g]	IC_{50} = 0.25 K_i = 0.04	> 100	EC_{50} = 30	EC_{50} = 38
5	Bz-(3-guani–dinyl)Phg-Arg-X	9.8%	IC_{50} = 0.26 K_i = 0.22	22%	IC_{50} = 0.14 K_i = 0.12	IC_{50} = 1.2	> 100	24%	47%
6	Bz-(3-guani–dinyl)Phe-Arg-X	IC_{50} = 211	IC_{50} = 0.11 K_i = 0.091	33%	IC_{50} = 0.31 K_i = 0.30	IC_{50} = 1.9	≥ 100	EC_{50} = 48	38%
7	Bz-(4-guani–dinyl)Phe-Arg-X	IC_{50} = 87 K_i = 29	IC_{50} = 0.036[f] K_i = 0.027[f]	34%	IC_{50} = 0.071[h] K_i = 0.065[h]	IC_{50} = 0.83	> 100	EC_{50} = 18	EC_{50} = 25
8	4-tBuBz-(4-guanidinyl)Phe-Arg-X	IC_{50} = 145	IC_{50} = 0.11[f] K_i = 0.078[f]	34%	IC_{50} = 0.21 K_i = 0.16	IC_{50} = 2.1	> 100	EC_{50} = 19	30%

All measurements were performed in triplicate. Standard deviations are always below 10%. Percentage inhibition values determined at 50 μM inhibitor concentration. K_i values were calculated from measurements at substrate concentrations of 50, 100, 150, and 200 μM. [a] Dengue serotype 2 NS2B-NS3 protease (100 nM unless stated otherwise). Substrate: 50 μM Abz-Nle-Lys-Arg-Arg-Ser-3-(NO_2)Tyr (K_m = 105 μM). [b] WNV NS2B-NS3 protease (150 nM unless stated otherwise). Substrate: 50 μM Abz-Gly-Leu-Lys-Arg-Gly-Gly-3-(NO_2)Tyr (K_m = 212 μM). [c] ZIKV NS2B-NS3 protease (5 nM). Substrate: 10 μM Bz-Nle-Lys-Lys-Arg-AMC (K_m = 18 μM). [d] Cytotoxicity was assayed up to a maximum concentration of 100 μM. [e] Plaque assay results for DENV and WNV. Percentage inhibition values at 50 μM or at the highest non-toxic inhibitor concentration. [f] 50 nM DENV protease. [g] 100 nM WNV protease. [h] 75 nM WNV protease.

As shown in Table 1, significant activity is restricted to compounds that contain the reversible-covalent boronic acid building block at the C-terminus, with the corresponding amides being practically inactive. Analogs of the most active compounds **4** and **7** with a C-terminal carboxylic acid were also inactive (Table S2). The second important factor is the basicity of the C-terminal residue: The ornithine-boronic acid derivative **1** is significantly less active than its arginine congener **2** at DENV protease, but slightly more active at WNV protease. Further extension by one additional, basic-lipophilic residue such as aminomethyl-phenylalanine (**4**) and guanidino-phenylalanine (**6**, **7**, **8**) lead to a dramatic increase in activity. A clear preference for a *para* substitution of the basic moiety is evident for all three viral proteases, revealing compounds **4** and **7** as the most active ones with nanomolar affinity. A more flexible phenylalanine moiety in P_2 is preferred compared to a truncated and rigified phenylglycine scaffold (**5** vs. **6**).

The reversible-covalent building block, however, always requires the presence of specific recognition elements, as evidenced by the relative inactivity of the monopeptide-boronic acids **1** and **2**. This is in agreement with a recent study that showed protein targets to be remarkably resistant against small electrophilic fragments which do not contain additional, specific molecular recognition elements.[22]

It is noteworthy that the affinity of the dipeptidic compound **7** (K_i = 0.027 μM) is in the same range as that of the previously reported tetrapeptidic inhibitor Bz-Nle-Lys-Arg-Arg-B(OH)$_2$ (reported K_i = 0.043 μM) against DENV protease. The boronic acid derivatives also compare favorably with the recently reported, much larger N-terminally capped, non-natural tripeptides that reach IC_{50} values of 18 and 50 nM at DENV and WNV protease, respectively (compound **83** in the reference).[15]

While in case of DENV and WNV proteases the selectivity between compounds **4** and **7** is limited, for ZIKV protease a remarkable preference towards compound **4** with the 4-aminomethyl-phenylalanine side chain in P_2 is evident. This indicates a very pronounced preference for lysine mimetics in P_2 and may guide the way towards highly affine ZIKV protease ligands.

A compelling comparison can be made for the most active boronic acids **4** and **7** and their respective amide congeners. For both compounds, replacement of the amide group by a reversible-covalent boronic acid function increases the affinity by a factor of 1000.

The broad inhibitory effect of these compounds against all analyzed viral proteases gives hope for a route towards pan-antiflaviviral drugs.

The cellular activities reflect the high in-vitro potencies, with the boronic acid **7** showing the highest activity against dengue protease in-vitro and DENV replication in cell culture. A single compound (**3**) had cytotoxic effects, probably due to the aniline moiety, with all other compounds being not cytotoxic up to 100 µM. Although this indicates good target selectivity, the inhibition data on trypsin (cf. SI) show that further improvements are required. In contrast, selectivity against thrombin is already relatively good. (cf. SI)

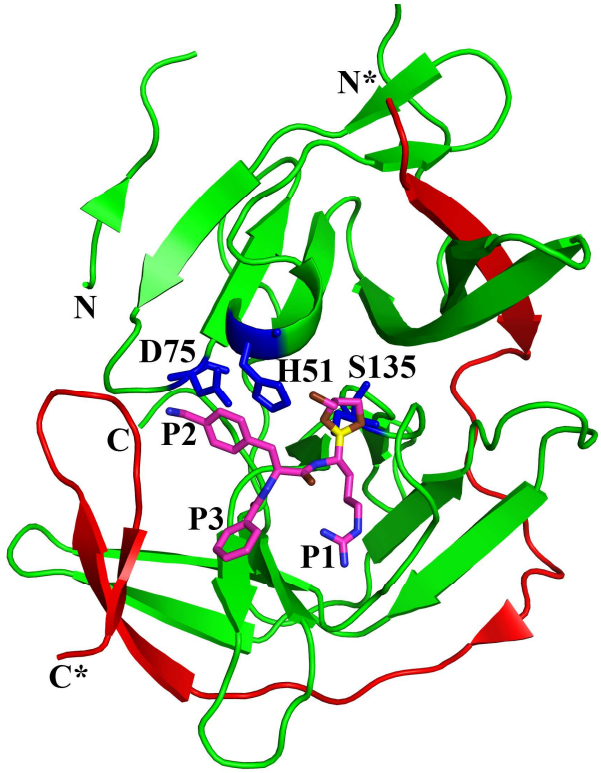

Figure 1. Overall structure of the WNV NS2B-NS3 protease in complex with compound **4**, PDB code 5IDK. A distinctive feature of the closed (active) form of the enzyme as found here is that the NS2B chain (red) is wrapped around the NS3 protease domain (green). The Gly_4-Ser-Gly_4 linker between NS2B and NS3 is not defined by electron density. Chain termini are labeled N*, C* for NS2B and N, C for NS3. Colors of inhibitor atoms: C, magenta; N, blue; O, dark red; B, yellow. Active-site residues are dark blue and labeled.

A 1.50-Å crystal structure of **4** in complex with the WNV NS2B-NS3 protease revealed the enzyme in the closed (active) conformation, with the NS2B chain wrapped around the NS3 domain (Fig. 1, PDB code 5IDK). The amide backbone of the inhibitor forms only two hydrogen bonds to the protease (P1 NH...Gly151 O, P3 O...Gly153 NH), whereas the P1 and P2 sidechains and the P3 benzoyl cap are neatly accommodated in the corresponding subsites of the enzyme (Fig. 2). The terminal NH_2 group of the P2 sidechain is involved in hydrogen bonds with the main-chain oxygen of Asp82* and with Asn84* Oδ1, both from the NS2B polypeptide chain. These interactions presumably contribute to the stabilization of the closed form of the complex.

Remarkably, the phenyl group of the P2 residue interacts with the imidazole of the catalytic His51 through π stacking (Fig. 2; distance ~3.5 Å). The Nε atom of the P1 guanidinium group is involved in a 2.97±0.08-Å hydrogen bond with the carbonyl oxygen of Tyr130, and the Nη2 donates a "charged" hydrogen bond to Asp129 Oδ1 (2.97±0.22 Å; average and standard deviation calculated from the 3 monomers of the complex in the asymmetric unit of the crystal). Interestingly, the Nη1 forms a 3.18±0.11-Å hydrogen bond with the carbonyl oxygen of the inhibitor's P2 residue, drawing the P1 guanidinium group close to the main chain of the compound. Moreover, there may be a weak (parallel) interaction between the guanidinium group and the phenyl group of Tyr161 (Fig. 2).

In contrast to a recently solved, lower resolution dimeric structure of compound **4** in complex with ZIKV protease (PDB code 5LC0), the present monomeric WNV crystal structure shows no evidence for specific contacts between two protease units, and no shape complementarity, as opposed to the crystal structure of the Zika virus NS2B-NS3 protease.[23] The overall observed inhibitor orientation in the active site is quite similar for both crystal structures (cf. SI Figure S1) and also in close correlation to an NMR structure of derivative **8** with DENV-2 protease.[24]

The boron atom of compound **4** forms a 1.59±0.01-Å covalent bond with Oγ of the active-site Ser135 (Fig. 2, upper right inset). During refinement, additional positive F_o–F_c density emerged near the two hydroxyl groups of the boronic acid and was unambiguously assigned to a cyclic di-ester formed between the boronic acid and atoms O1 and O2 of glycerol, leading to the formation of a 5-membered ring (Fig. 2, lower left inset). Boronic acids tend to form esters with aliphatic diols, especially if 5- or 6-membered rings can be formed,[25] and glycerol was present in our enzyme preparation during purification, crystallization, and cryoprotection of crystals.

The presence of alcohols (e.g., TRIS) and polyols in biological and biochemical assays leads to formation of an equilibrium mixture of boronate esters and boronic acids. For example, the formation of a TRIS ester under assay conditions was detected for a representative compound of the current dataset by mass spectrometry (data not shown). The kinetics and dynamics of these ester/acid equilibria are not yet well characterized, neither for the currently presented compounds nor for the clinically used boronic acids. Affinity data for boronic acid electrophiles must therefore be interpreted with caution, because the composition of buffers and biological media influences the concentration of the "active", free boronic acid.

Negatively charged and chiral, the tetrahedral boronate unit is a close mimic of the transition state of peptide hydrolysis. The cyclic-ester oxygens (O1 and O2) accept hydrogen bonds from the amide of Gly133 (2.85±0.05 Å;

part of the oxyanion hole) and the Nε2 of His51 (2.67±0.04 Å), respectively. The five-membered ring occupies the S1' site, but the hydroxy group (O3 of glycerol) is oriented towards bulk solvent.

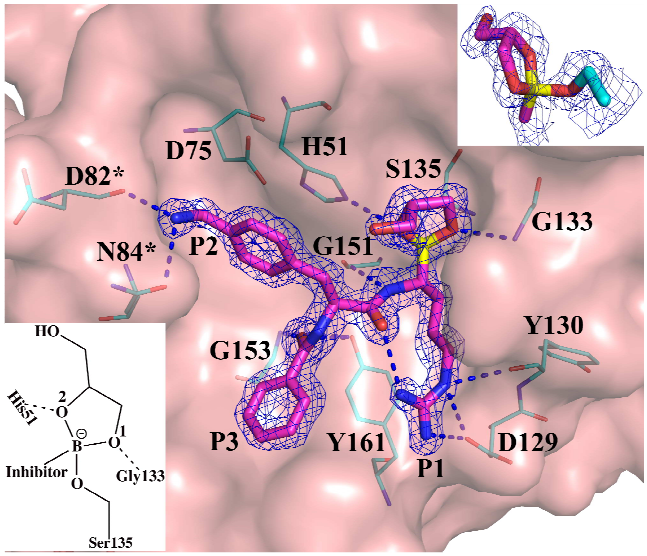

Figure 2. Compound **4** in the substrate-binding site of WNV NS2B-NS3 protease. The F_o-F_c difference density, calculated from the final coordinates with the inhibitor omitted and contoured at 4σ, is shown as blue grid. Residues of the NS2B chain are indicated by an asterisk (*). H-bonds are shown as dashed lines. Upper right inset: The tetrahedral boronate; Ser135 in green, boron in yellow, oxygens and carbons of the glycerol moiety in red, Fo-Fc difference density as blue grid. Lower left inset: Structure of the glycerol boronate bound to Ser135.

The structure presented here has the highest resolution of all flavivirus protease structures in complex with a small-molecule inhibitor published thus far and will enable us and others to further optimize target affinity and selectivity of flaviviral protease inhibitors.

Some key consequences for drug design shall be summarized here: Several backbone atoms of the inhibitor are not engaged in interactions with the protease and may therefore be replaced in order to reduce the peptidic nature of the inhibitor. This relates in particular to the P2 main-chain amide, which could be replaced by a methylene group or a similar functionality, allowing the creation of peptidomimetics with increased drug-likeness. A ring closure between the P2 main-chain carbonyl and the P1 side-chain appears possible and would reduce the conformational degrees of freedom of the inhibitor, thus further increasing affinity.

The structure also highlights significant opportunities to further extend these inhibitors in a rational way, not only with respect to target affinity but also in light of selectivity: Most prominently, the glycerol ester indicates that inhibitors can be extended towards the prime-sites of the substrate-binding cleft, which so far remain completely unexploited. The P2 and P3 regions offer significant potential for the design of additional specific interactions with side chains of the target and, more importantly, towards the protein backbone. Creation of additional protein backbone – inhibitor interactions would be highly attractive since this is expected to impede resistance development and increase the likelihood of broad-spectral activity against proteases from multiple flaviviruses.

An unresolved issue is the relatively weak activity of the compounds in the virus replication assay, and the lack of correlation between the cellular and the biochemical activity of the compounds. We assume that the high polarity of the compounds, not only due to the basic side chains but also to the boronic acid moiety, impedes membrane passage, and thus, cellular uptake of the compounds. In this respect, the boronic acid moiety, while contributing significantly to target affinity, probably has a detrimental effect. Therefore, while the value of the present compounds for structural and biochemical studies is high – such as successfully shown for the protease of the newly emerged Zika virus[23] – modifications will be required to reach higher antiviral efficacy in cells. We envisage that this can be reached via two strategies: First, the boronic acid might be modified to a prodrug, for example by esterification with diols, yielding compounds that resemble the inhibitor-glycerol complex as found in the present X-ray structure. Second, the boronic acid might be replaced by other electrophilic functional groups with lower polarity. Alternative functional groups such as the fluoromethylketone moiety would furthermore allow the extension of the inhibitors towards the primed sites. This may increase selectivity towards flaviviral proteases in relation to eukaryotic off-targets such as trypsin and thrombin, which remains problematic for the compounds presented here.

In conclusion, the current study not only contributes to our understanding of flaviviral proteases and their substrate and inhibitor binding mechanisms, but also supports the ongoing search for novel therapeutics to treat infections with dengue, West Nile, Zika and other emerging flaviviruses.

EXPERIMENTAL SECTION

General Procedures. Detailed information are provided in the Supporting Information. In brief, all reagents and solvents were used as obtained from commercial sources unless otherwise indicated. Sensitive reagents were generally handled under nitrogen atmosphere. The reaction progress was monitored by TLC. Normal phase chromatographic purification was performed on a Biotage Isolera One purification system using silica gel and UV monitoring. RP-phase purifications were executed using an ÄKTA purifier (GE Healthcare) system with Reprospher C18-DE, Dr. Maisch (5 µm) 30 x 16 mm, and 120 x 16 mm pre- and main columns and UV detection. NMR spectra were recorded on Varian Mercury Plus (300 MHz) and Varian NMR System 500 (500 MHz) instruments at 300 K. Mass spectrometry was performed on a Bruker micrOTOF-Q II (ESI) instrument. Analytical HPLC was performed on a Jasco HPLC system with UV detector and ReproSil-Pur-ODS-3, Dr. Maisch GmbH, Germany, 5 µm, 50 x 2 mm

column. Active compounds **3**-**8** were of ≥95% purity according to HPLC analysis.

Synthesis of precursor 9. Compound **9** was synthesized from allyl bromide in 4 steps according to the literature[21] (5.60 g, 64%, final step). ^{1}H-NMR (300 MHz, $CDCl_3$): δ = 0.85 (s, 3H), 0.98 (t, *J* = 7.4 Hz, 2H), 1.10 (d, *J* = 10.9 Hz, 1H), 1.30 (s, 3H), 1.39 (s, 3H), 1.80-2.07 (m, 5H), 2.23 (m, 1H), 2.33 (m, 1H), 3.45 (t, *J* = 6.9 Hz, 2H), 4.27 (dd, *J* = 8.7, 2.0 Hz, 1H) ppm; ^{13}C-NMR (75 MHz, $CDCl_3$): δ = 24.0, 26.5, 27.1, 27.6, 28.6, 35.5, 36.3, 38.1, 39.5, 51.3, 77.7, 85.6 ppm; MS (ESI): *m*/*z*: 323.1 $[M+Na]^+$.

Synthesis of precursor amino acid 11. Compound **11** was synthesized from L-4-cyanophenylalanine in 5 steps following established synthetic procedures (442 mg, 93%, final step). ^{1}H-NMR (300 MHz, $CDCl_3$): δ = 7.72 (d, *J* = 7.1 Hz, 2H), 7.38-7.61 (m, 4H), 7.32 (d, *J* = 8.2 Hz, 1H), 7.05-7.16 (m, *J* = 6.8 Hz, 2H), 6.69 (br s, 1H), 5.03-5.16 (m, 1H), 4.29 (s, 1H), 3.23-3.53 (m, 2H), 1.46 (s, 6H) ppm; HRMS (ESI): *m*/*z* $[M-H]^-$ calcd for $C_{22}H_{25}N_2O_5$: 397.1769, found: 397.1770.

Synthesis of 4. A solution of **11** (200 mg, 0.5 mmol) and *N*-methylmorpholine (60 µl, 0.55 mmol) was dissolved in THF and cooled to -15 °C, before IBCF (130 µl, 1 mmol) was added. Afterwards a solution of **9** (220 mg, 0.6 mmol) in dichloromethane was added dropwise, followed by a slightly delayed addition of DIPEA (190 µl, 1.1 mmol) in dichloromethane at -15 °C over 30 min. Afterwards, the reaction mixture was allowed to warm up to room temperature and stirred overnight. The solvent was evaporated and the residue was purified by flash chromatography (cyclohexane/ethyl acetate) to obtain a crude intermediate (59%). HRMS (ESI): *m*/*z* $[M+Na]^+$ calcd for $C_{36}H_{49}BBrN_3NaO_6$: 732.2796, found: 732.2789. The intermediate (320 mg, 0.45 mmol) was treated with sodium azide (39 mg, 0.6 mmol) in DMF at 100 °C for 1 h. Afterwards, the solvent was evaporated and the residue was purified by flash chromatography (cyclohexane/ethyl acetate) to obtain a crude product (79%). HRMS (ESI): *m*/*z* $[M+Na]^+$ calcd for $C_{36}H_{49}BN_6NaO_6$: 695.3705, found: 695.3712. A mixture of this intermediate (220 mg, 0.33 mmol) and palladium on carbon (10%, 35 mg) in methanol was stirred at room temperature under hydrogen atmosphere (1 bar) overnight. The mixture was filtered using celite, the solvent was evaporated and the crude product was directly used for the next synthetic step (200 mg, 94%). HRMS (ESI): *m*/*z* $[M+H]^+$ calcd for $C_{36}H_{52}BN_4O_6$: 647.3981, found: 647.3957. A solution of the crude intermediate (195 mg, 0.3 mmol), bis-Boc-pyrazole-1-carboxamidine (116 mg, 0.375 mmol) and DMAP (10 mg, 0.075 mmol) in methanol was stirred 2 days at room temperature. The solvent was evaporated and the residue was purified by flash chromatography (cyclohexane/ethyl acetate) to obtain a crude product (175 mg, 66%). HRMS (ESI): *m*/*z* $[M+H]^+$ calcd for $C_{47}H_{70}BN_6O_{10}$: 889.5249, found: 889.5228. The intermediate (160 mg, 0.18 mmol) was treated with a mixture of dichloromethane (10 ml) and TFA (1 ml) overnight. After solvent evaporation, the residue was triturated with hydrogen chloride (1 ml, 4 M in dioxane) and the solvent was evaporated again to obtain a crude intermediate (120 mg, quant.). HRMS (ESI): *m*/*z* $[M+H]^+$ calcd for $C_{32}H_{46}BN_6O_4$: 589.3674, found: 589.3672. The residue was stirred overnight in a two-phase mixture of water and diethyl ether containing phenylboronic acid (109 mg, 0.9 mmol). Afterwards, the phases were separated and the aqueous phase was extracted with diethyl ether for three times. The aqueous phase was concentrated and directly used for purification by preparative HPLC (methanol/water 0.1% TFA). The excess of methanol was evaporated and hydrochloric acid (1 ml, 1N) was added before freeze-drying. Compound **4** was obtained as colorless solid (15 mg, 16%). ^{1}H-NMR (500 MHz, D_2O): δ = 1.38-1.54 (m, 4H), 2.65 (m, 1H), 3.13 (t, *J* = 6.8 Hz, 2H), 3.17 (dd, *J* = 13.9, 9.5 Hz, 1H), 3.33 (dd, *J* = 13.8, 6.4 Hz, 1H), 4.12 (s, 2H), 4.96 (dd, *J* = 9.5, 6.5 Hz, 1H), 7.38 (m, 4H), 7.27 (m, 2H), 7.61 (m, 3H) ppm; ^{13}C-NMR (125 MHz, D_2O): δ = 25.8, 27.1, 36.3, 40.9, 42.7, 52.8, 127.1, 128.7, 129.1, 129.9, 131.4, 132.5, 132.6, 137.2, 170.9, 174.8 ppm; HRMS (ESI): *m*/*z* $[M-H_2O+H]^+$ calcd for $C_{22}H_{30}BN_6O_3$: 437.2471, found: 437.2463.

ASSOCIATED CONTENT

Supporting Information. Detailed biochemical and chemical procedures, structures of all intermediates, biochemical and analytical data, details of the crystallisation, X-ray data collection, and refinement. This material is available free of charge via the Internet at http://pubs.acs.org.

AUTHOR INFORMATION

Corresponding Author

*E-mail: c.klein@uni-heidelberg.de. Phone: ++49-6221-544875.

Present Address

‡C.N.: Australian National University, Research School of Chemistry, Canberra, ACT 2601, Australia

Funding Sources

The project was supported by the Deutsche Forschungsgemeinschaft, KL-1356/3-1, and by the German Center for Infection Research (DZIF), 8029801911.

ACKNOWLEDGMENT

We thank Dr. Tom Sundermann, Heiko Rudy, Tobias Timmermann, Natascha Stefan and Yasmin Gül for support. Dr. Mascha Jäkel kindly provided (+)-pinanediol. Dr. Mira A. M. Behnam and Dr. Daizong Lin were valuable partners for discussions.

ABBREVIATIONS

DENV, dengue virus; WNV, West Nile virus; ZIKV, Zika virus; NS2B, non-structural protein 2B; NS3, non-structural protein 3.

PDB ID CODES

Atomic coordinates of the WNV NS2B-NS3 protease in complex with compound **4** will be released upon acceptance of the article, PDB code 5IDK.

REFERENCES

1. Smith, A. J.; Zhang, X.; Leach, A. G.; Houk, K. N. Beyond picomolar affinities: Quantitative aspects of noncovalent and covalent binding of drugs to proteins. *J. Med. Chem.* **2009,** *52*, 225-233.
2. Li, D.; Ambrogio, L.; Shimamura, T.; Kubo, S.; Takahashi, M.; Chirieac, L. R.; Padera, R. F.; Shapiro, G. I.; Baum, A.; Himmelsbach, F.; Rettig, W. J.; Meyerson, M.; Solca, F.; Greulich, H.; Wong; K, K. BIBW2992, an irreversible EGFR/HER2 inhibitor highly effective in preclinical lung cancer models. *Oncogene* **2008,** *27*, 4702-4711.
3. Weisner, J.; Gontla, R.; van der Westhuizen, L.; Oeck, S.; Ketzer, J.; Janning, P.; Richters, A.; Mühlenberg, T.; Fang, Z.; Taher, A.; Jendrossek, V.; Pelly, S. C.; Bauer, S.; van Otterlo, W. A. L.; Rauh, D. Covalent-allosteric kinase inhibitors. *Angew. Chem. Int. Ed.* **2015,** *54*, 10313-10316.
4. Dubiella, C.; Baur, R.; Cui, H.; Huber, E. M.; Groll, M. Selective inhibition of the immunoproteasome by structure-based targeting of a non-catalytic cysteine. *Angew. Chem. Int. Ed.* **2015,** *54*, 15888-15891.
5. Adams, J.; Palombella, V. J.; Sausville, E. A.; Johnson, J.; Destree, A.; Lazarus, D. D.; Maas, J.; Pien, C. S.; Prakash, S.; Elliott, P. J. Proteasome inhibitors: A novel class of potent and effective antitumor agents. *Cancer Res.* **1999,** *59*, 2615-2622.
6. Hecker, S. J.; Reddy, K. R.; Totrov, M.; Hirst, G. C.; Lomovskaya, O.; Griffith, D. C.; King, P.; Tsivkovski, R.; Sun, D.; Sabet, M.; Tarazi, Z.; Clifton, M. C.; Atkins, K.; Raymond, A.; Potts, K. T.; Abendroth, J.; Boyer, S. H.; Loutit, J. S.; Morgan, E. E.; Durso, S.; Dudley, M. N. Discovery of a cyclic boronic acid β-lactamase inhibitor (rpx7009) with utility vs class A serine carbapenemases. *J. Med. Chem.* **2015,** *58*, 3682-3692.
7. Nitsche, C.; Schreier, V. N.; Behnam, M. A. M.; Kumar, A.; Bartenschlager, R.; Klein, C. D. Thiazolidinone–peptide hybrids as dengue virus protease inhibitors with antiviral activity in cell culture. *J. Med. Chem.* **2013,** *56*, 8389-8403.
8. Hammamy, M. Z.; Haase, C.; Hammami, M.; Hilgenfeld, R.; Steinmetzer, T. Development and characterization of new peptidomimetic inhibitors of the West Nile virus NS2B–NS3 protease. *ChemMedChem* **2013,** *8*, 231-241.
9. Nitsche, C.; Behnam, M. A. M.; Steuer, C.; Klein, C. D. Retro peptide-hybrids as selective inhibitors of the dengue virus NS2B-NS3 protease. *Antiviral Res.* **2012,** *94*, 72-79.
10. Stoermer, M. J.; Chappell, K. J.; Liebscher, S.; Jensen, C. M.; Gan, C. H.; Gupta, P. K.; Xu, W.-J.; Young, P. R.; Fairlie, D. P. Potent cationic inhibitors of West Nile virus NS2B/NS3 protease with serum stability, cell permeability and antiviral activity. *J. Med. Chem.* **2008,** *51*, 5714-5721.
11. Schüller, A.; Yin, Z.; Brian Chia, C. S.; Doan, D. N. P.; Kim, H.-K.; Shang, L.; Loh, T. P.; Hill, J.; Vasudevan, S. G. Tripeptide inhibitors of dengue and West Nile virus NS2B–NS3 protease. *Antiviral Res.* **2011,** *92*, 96-101.
12. Leung, D.; Schroder, K.; White, H.; Fang, N.-X.; Stoermer, M. J.; Abbenante, G.; Martin, J. L.; Young, P. R.; Fairlie, D. P. Activity of recombinant dengue 2 virus NS3 protease in the presence of a truncated NS2B co-factor, small peptide substrates, and inhibitors. *J. Biol. Chem.* **2001,** *276*, 45762-45771.
13. Behnam, M. A. M.; Nitsche, C.; Vechi, S. M.; Klein, C. D. C-Terminal residue optimization and fragment merging: Discovery of a potent peptide-hybrid inhibitor of dengue protease. *ACS Med. Chem. Lett.* **2014,** *5*, 1037-1042.
14. Bastos Lima, A.; Behnam, M. A. M.; El Sherif, Y.; Nitsche, C.; Vechi, S. M.; Klein, C. D. Dual inhibitors of the dengue and West Nile virus NS2B–NS3 proteases: Synthesis, biological evaluation and docking studies of novel peptide-hybrids. *Bioorg. Med. Chem.* **2015,** *23*, 5748-5755.
15. Behnam, M. A. M.; Graf, D.; Bartenschlager, R.; Zlotos, D. P.; Klein, C. D. Discovery of nanomolar dengue and West Nile virus protease inhibitors containing a 4-benzyloxyphenylglycine residue. *J. Med. Chem.* **2015,** *58*, 9354-9370.
16. Weigel, L. F.; Nitsche, C.; Graf, D.; Bartenschlager, R.; Klein, C. D. Phenylalanine and phenylglycine analogues as arginine mimetics in dengue protease inhibitors. *J. Med. Chem.* **2015,** *58*, 7719-7733.
17. Yin, Z.; Patel, S. J.; Wang, W.-L.; Wang, G.; Chan, W.-L.; Rao, K. R. R.; Alam, J.; Jeyaraj, D. A.; Ngew, X.; Patel, V.; Beer, D.; Lim, S. P.; Vasudevan, S. G.; Keller, T. H. Peptide inhibitors of dengue virus NS3 protease. Part 1: Warhead. *Bioorg. Med. Chem. Lett.* **2006,** *16*, 36-39.
18. Matteson, D. S. Boronic esters in asymmetric synthesis. *J. Org. Chem.* **2013,** 78, 10009-10023.
19. Matteson, D. S.; Ray, R. Directed chiral synthesis with pinanediol boronic esters. *J. Am. Chem. Soc.* **1980,** *102*, 7590-7591.
20. Matteson, D. S.; Sadhu, K. M. Boronic ester homologation with 99% chiral selectivity and its use in syntheses of the insect pheromones (3S,4S)-4-methyl-3-heptanol and exo-brevicomin. *J. Am. Chem. Soc.* **1983,** *105*, 2077-2078.
21. Wityak, J.; Earl, R. A.; Abelman, M. M.; Bethel, Y. B.; Fisher, B. N.; Kauffman, G. S.; Kettner, C. A.; Ma, P.; McMillan, J. L. Synthesis of thrombin inhibitor DuP 714. *J. Org. Chem.* **1995,** *60*, 3717-3722.
22. Jöst, C.; Nitsche, C.; Scholz, T.; Roux, L.; Klein, C. D. Promiscuity and selectivity in covalent enzyme inhibition: A systematic study of electrophilic fragments. *J. Med. Chem.* **2014,** *57*, 7590-7599.
23. Lei, J.; Hansen, G.; Nitsche, C.; Klein, C. D.; Zhang, L.; Hilgenfeld, R. Crystal structure of Zika virus NS2B-NS3 protease in complex with a boronate inhibitor. *Science* **2016,** *353*, 503-505.
24. Chen, W. N.; Nitsche, C.; Pilla, K. B.; Graham, B.; Huber, T.; Klein, C. D.; Otting, G. Sensitive NMR approach for determining the binding mode of tightly binding ligand molecules to protein targets. *J. Am. Chem. Soc.* **2016,** *138*, 4539-4546.
25. Türker, L. Some boric acid esters of glycerol - An *ab initio* treatment. *Indian J. Chem.* **2006,** *45A*, 1339-1344.

TOC graphic

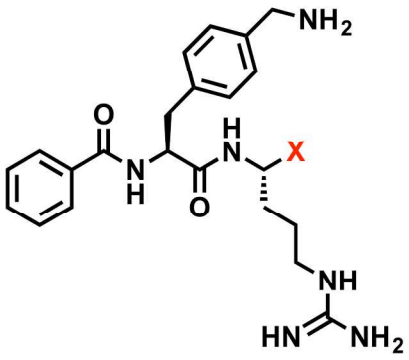

Protease inhibition *in vitro*

X = $B(OH)_2$

Dengue K_i = 0.051 μM

West Nile K_i = 0.082 μM

Zika K_i = 0.040 μM

X = CO_2H, $CONH_2$

K_i > 100 μM

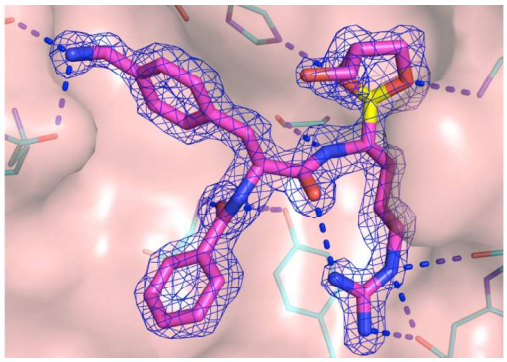

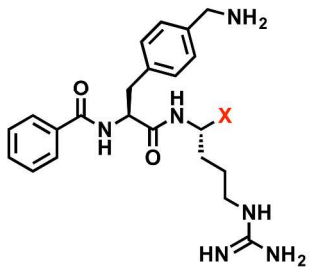

Protease inhibition *in vitro*

X = $B(OH)_2$
Dengue K_i = 0.051 μM
West Nile K_i = 0.082 μM
Zika K_i = 0.040 μM

X = CO_2H, $CONH_2$
K_i > 100 μM

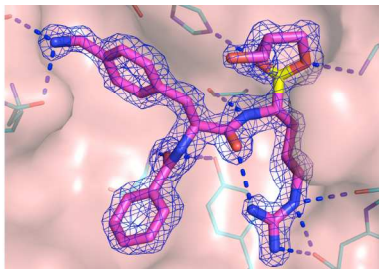

TOC GRAPHIC

1212x319mm (72 x 72 DPI)